Cubic magnetic anisotropy of nonstoichiometric magnetite

Ricardo Aragón
Department of Chemical Engineering, University of Delaware, Newark, Delaware 19716
(Received 6 August 1991; revised manuscript received 8 January 1992)

The cubic magnetic anisotropy constants of $Fe_{3(1-\delta)}O_4$ single crystals (with $0.000<\delta<0.006$), obtained by curve fitting of the respective magnetization curves, are reported between room temperature and the isotropic point (~ 130 K), where the easy axis changes from [111] to [100]. Two distinct temperature dependences are observed for nonstoichiometries above and below $\delta_C=0.0039$, in samples with second- and first-order Verwey transitions, respectively. The characteristic temperatures for the first-derivative curves are consistent with mean-field parameters for nearest-neighbor-interaction models.

I. INTRODUCTION

Numerous[1] prior experimental investigations have addressed the magnetocrystalline anisotropy of magnetite ($Fe_{3(1-\delta)}O_4$), the type material for Néel ferrimagnetism, motivated by the technological importance of the ferrite solid solutions, as well as by its possible connection to the charge-ordering phenomena associated with the Verwey[2] phase transition.

It is well established that small departures from nominal metal-oxygen stoichiometry can have profound effects on the physical properties of transition-metal oxides. This influence is dramatically illustrated by the sudden loss of the latent heat of the Verwey transition at $\delta_C=0.0039$ in a discontinuous change in character from first- to second-order behavior.[3]

Recent studies[4] of the influence of nonstoichiometry on the magnetic properties of magnetite have found no evidence of a discontinuous change in behavior at δ_C, which is difficult to reconcile with the existence of a unique ordering contribution to the thermodynamic potential. Consequently, the present work reexamines the thermal dependence of magnetic anisotropy in first- and second-order transition regimes—above T_V, to avoid complications from possible subtle structural differences in the low-temperature phases—with particular attention to thermodynamic consistency.

II. EXPERIMENTAL DETAILS

Three $Fe_{3(1-\delta)}O_4$ single crystals, grown[5] by rf induction melting from 99.999%-pure Fe_2O_3 reagent, were annealed[6] under controlled oxygen fugacity conditions, by techniques described elsewhere[5,6] to produce δ values of 0.000 and 0.003, respectively, corresponding to stoichiometric and cation-deficient samples with first-order Verwey transitions, and $\delta=0.006$, to induce cation deficiency beyond the critical value 0.0039, for which second-order Verwey transitions are observed.[3] The crystals were ground in a diamond abrasive air mill to spheres of 3–5 mm diameter, with sphericity of 10^{-2}, oriented by Laue back-reflection x-ray techniques on the cubic [100] axis, within 1°, and rigidly mounted with epoxy on quartz tubing.

Magnetization was measured in a superconducting quantum interference device (SQUID) magnetometer (Quantum Design MPMS2), as a function of applied fields between 200 Oe and 10 kOe, at temperatures between 125 and 300 K, after cooling in a 10-kOe field, applied parallel to the [100] mounting axis. Scan lengths of 3 cm were used, and the calibration was verified with a Pd standard; the effect of field inhomogeneity was evaluated with a Ni standard. Absolute accuracy was better than 1%, and the precision for six independent scans at each field was 0.1%.

Demagnetization factors (N_d), evaluated from the initial slopes of the magnetization curves for each temperature, were consistent to within 0.01% for 35 independent fits on each sample and in the range $4.2<N_d<4.3$, commensurate with the ideal sphere value of 4.189, within the stated sphericity for samples of this size.

A. Data reduction

The magnetocrystalline anisotropic energy per unit volume (W_A) of cubic crystals, expanded to second order, in terms of the direction cosines (l,m,n) of the magnetization vector (M_S) with respect to each cubic axis, is[7]

$$W_A=K_0+K_1(l^2m^2+m^2n^2+n^2l^2)+K_2(lmn)^2 , \quad (1)$$

where K_0 is independent of direction, whereas K_1 and K_2 contain the directional-preference information.

For magnetite above the isotropic point, [111] is the easy magnetization direction (i.e., $K_1<0$ and $0<K_2<1.2K_1$). Let γ be the angle of the magnetic moment with respect to an applied field along [001]; then the energy-minimization condition $dW/d\gamma=0$, applied to Eq. (1), in terms of the fractional magnetization ($a=M/M_S$) yields,[8] factored for data reduction,

$$H_{\text{eff}}M_S=-K_1(3a^3-a)+\frac{K_2}{2}(3a^5-4a^3+a) , \quad (2)$$

to obtain K_1 and K_2, from the measured magnetization and effective field (H_{eff}), obtained by subtraction of the demagnetizing (N_dM) from the applied field, by a singular value decomposition solution of the corresponding least-squares problem,[9] excluding the low- and high-field

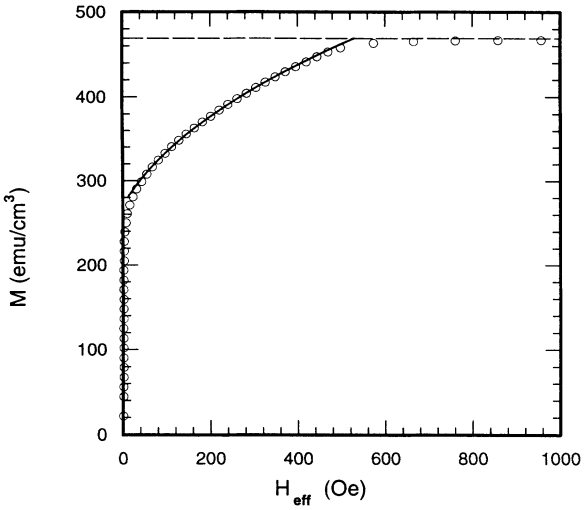

FIG. 1. Representative fit (solid line) of magnetization vs effective-field data (circles) for a first-order sample at 300 K and saturation limit (dashed line).

regions, with valid data restricted to the $0.65 < a < 0.85$ range. A representative sample fit is shown in Fig. 1.

III. RESULTS AND DISCUSSION

The fitted values of the K_1 anisotropy constant for each crystal (cf. Fig. 2) are in general agreement with previously reported torque measurements.[10] Two distinct regimes are apparent for samples with δ above and below $\delta_C = 0.0039$.

For $\delta < \delta_C$, in samples with first-order Verwey transitions,[3] the values of K_1 at each measured temperature ($130 < T < 300$ K) are mostly indistinguishable (cf. Fig. 2) within experimental uncertainty ($\pm 2\%$).

The thermal dependence of K_1^{II} for $\delta > \delta_C$ (cf. Fig. 2), in the second-order Verwey-transition regime, diverges from that of the first-order transition below $\cong 225$ K (i.e., $K_1^{II} < K_1^{I}$; cf. Fig. 2), leading to a lower isotropic point (125 K) than that characteristic for $\delta < \delta_C$ (130 K). Above $\cong 225$ K, the reverse inequality is verified, i.e., $K_1^{II} > K_1^{I}$. Below 180 K the steep dependence of K_1 on temperature induces differences $K_1^{II} - K_1^{I}$, which are one to two orders of magnitude larger than the experimental uncertainty.

The net effect, associated with the change from the first- to second-order T_V regime, for $\delta > \delta_C$, amounts to a discontinuous displacement of the respective K_1-vs-T curve by 5 K. Kakol, Pribble, and Honig[4] have reported, instead,[11] a uniform reduction of the magnitude of K_1 with δ (from -1.2×10^5 to -1.0×10^5 erg/cm^3 at room temperature), convergent on a unique isotropic point at 130 K.

In all cases the anisotropy constant K_2 is negative and obeys a thermal dependence similar to K_1; however, the uncertainties of the fitted values are at least an order of magnitude greater, rendering further consideration speculative.

A. Magnetic anisotropy and Verwey ordering

It has long been recognized[12] that an intimate connection exists between the dramatic drop in anisotropy from 250 K to the isotropic point at 130 K and the subsequent Verwey transition ($T_V < 122$ K). In an attempt to parametrize this relation, a procedure similar to that used to account for the effects of Co doping[13] has been applied[10] to distinguish the ordering-related term from all other contributions to K_1. The necessary mapping relies on the fact that the monoclinic low-temperature anisotropy constants, reduced by their projection on the cubic crystallographic axis, to obtain an effective cubic K_1 constant below T_V, lie on a common base line with the measured[14] high-temperature ($250 < T < 800$ K) K_1 values (cf. Fig. 3). The contribution of Verwey ordering to anisotro-

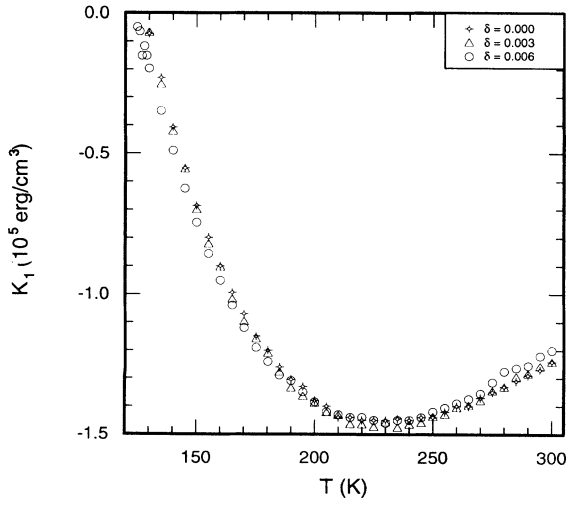

FIG. 2. K_1 anisotropy constants for samples with $\delta = 0.000$ (stars), 0.003 (triangles), and 0.006 (circles).

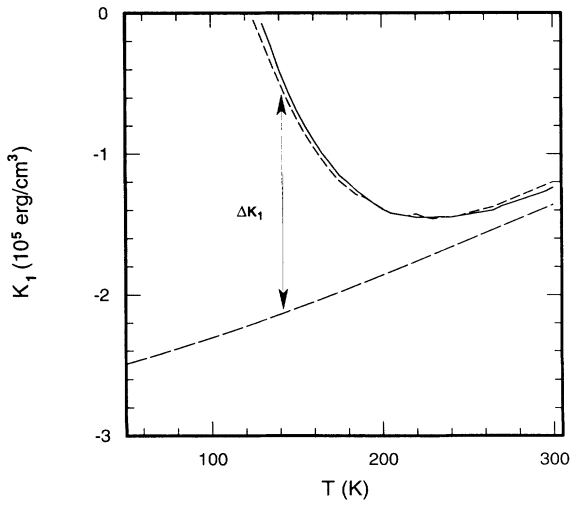

FIG. 3. Experimental K_1 anisotropy in first-order (solid line) and second-order (short-dashed line) Verwey-transition regimes and reference base line (long-dashed line) from Ref. 10, with an indication of the ΔK_1 variable.

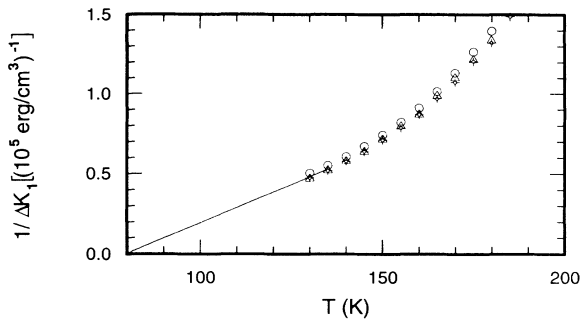

FIG. 4. Inverse ΔK_1 plot for $\delta=0.000$ (stars), 0.003 (triangles), and 0.006 (circles) and its extrapolation to zero at 81 K (indicated by a straight-line approximation).

py is thus empirically parametrized by a new variable: ΔK_1, obtained from the difference between the experimental and base-line values at each temperature. However, further fittings of ΔK_1 in terms of single-ion functions yield unrealistically low concentrations of anisotropic cations.[10]

It has been noted[15] empirically that the reciprocal of ΔK_1 vanishes at 81 K, analogously to the behavior of the c_{44} elastic modulus. This simple relation is satisfied by both first- and second-order T_V samples (cf. Fig. 4), although the linearity is compromised by a sensitive dependence on the extrapolated base line. The physical interpretation of this functional dependence is readily apparent on thermodynamic principles, with due recognition that the anisotropic energy [cf. Eq. (1)] represents a contribution to the Helmholtz potential. Indeed, in Slonzewski's approximation,[13] the cubic anisotropy constant is represented by

$$K_1=4(F[110]-F[100]) , \tag{3}$$

where $F[hkl]$ are magnetocrystalline anisotropy components of the Helmholtz potential on the appropriate crystallographic directions. The subtraction of a continuous base line implies the adoption of a hypothetical reference thermodynamic state without Verwey ordering and ΔK_1, merely the corresponding excess property, which is necessarily singular at the transition. The advantage of examining the difference in an equilibrium physical property between two thermodynamic states is that the thermal dependence intrinsic to that property, which is model dependent, cancels out, leaving only the thermal dependence of the excess potential, described by a function of the appropriate long-range-order parameter. To understand the behavior of ΔK_1 in the neighborhood of the transition, it suffices to characterize that of the order parameter. In this context the linearity of ΔK_1^{-1} with T implies a Curie-Weiss-type law[16]

$$\Delta K_1 \propto (T-\Theta)^{-1} , \tag{4}$$

characteristic of the second-order (T_V^{II}) regime with $\Theta=81$ K.

B. Mean-field model

The formal representation of the general thermodynamic considerations of the previous section finds its simplest expression in the mean-field approximation. In a previous communication,[17] it was shown that, accounting for the splitting of electronic states in the first-order Verwey-transition regime for $\delta<\delta_C$, the simple equation of state proposed by Strässler and Kittel,[18]

$$\varepsilon-\lambda\Psi-k_BT\left[\ln\left[\frac{g_1}{g_0}\right]+\ln\left[\frac{1-\Psi}{\Psi}\right]\right]=0 , \tag{5}$$

in terms of noninteracting (ε) and interacting (λ) contributions to the internal energy of a fraction of excited states of degeneracy g_1 and ground states of degeneracy g_0, characterized by a single long-range-order parameter (Ψ), provides a complete thermodynamic description of the dependence of Verwey ordering on nonstoichiometry (δ) by its influence on the magnitude of the interactions (λ).

The equation of state [cf. Eq. (5)] can be mapped to the canonical cusp catastrophe with the diffeomorphism obtained by reduction of all variables $(\varepsilon,\lambda,\Psi,T)$ to new coordinates (e,l,r,t), with a change of origin to δ_C, where the discontinuous change from a first- to second-order transitions occurs. The resulting critical manifold[19]

$$r^3-3lr+3\left\{e\left[1+\frac{1}{2}\ln\left[\frac{g_1}{g_0}\right]\right]-l\right\}=0 , \tag{6}$$

where

$$e\left[1+\frac{1}{2}\ln\left[\frac{g_1}{g_0}\right]\right]-l=\frac{1}{2}\frac{T_V-T}{T}\ln\left[\frac{g_1}{g_0}\right]=\frac{1}{2}t\ln\left[\frac{g_1}{g_0}\right] ,$$

plotted in Fig. 5, contains all the topological information necessary to relate the thermal dependencies of any physical property[20] in first- and second-order regimes by the respective degeneracy ratios (g_1/g_0), namely, 2 and 1.

The reduction of variables permits the representation of all Verwey critical behavior on a common control space (i.e., t vs l). The Curie-Weiss dependence [Eq. (4)] will be applicable to all second-order transitions, namely, the contiguous set of T_V^{II}, for which $g_1/g_0=1$, and the isolated second-order transition at the nose of the first-order cusp, for which $g_1/g_0=2$. The formal equivalence of Eq. (5) with the Weiss equation of state in these cases was proved in Ref. 17. The intersection of the first-order (T_V^{I}) and second-order (T_V^{II}) transition temperatures plotted with respect to nonstoichiometry (δ), which is a linear mapping of l, occurs at 81 K, below which the interactions (i.e., λ or l) are too weak to induce ordering. Hence the common characteristic temperature $\Theta=81$ K for all Curie-Weiss dependencies plotted in Fig. 4 represents the invariant at the pivot point of the first- and second-order cusps.

A much stronger topological constraint can be ob-

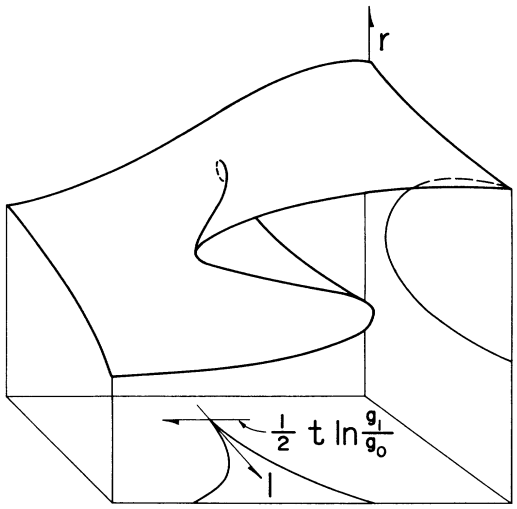

FIG. 5. Schematic representation of the cusp critical manifold and its projections; r is the reduced order parameter, l the reduced interaction variable, t the reduced temperature, and g_0 and g_1 the degeneracies of the ground and excited states (reproduced from Ref. 17).

tained by examining the contribution to the Helmholtz potential due to the internal-energy parameter (ε or e) associated with the splitting of degeneracies in the first-order regime. All that is required is a change of the reference state, from one without Verwey ordering, as used in the definition of ΔK_1, to one of equal degeneracy. The empirical quantity which provides the appropriate function of the order parameters is then $(K_1^{\mathrm{I}}-K_1^{\mathrm{II}})$. Equation (6) predicts that the first-order cusp is pivoted by $\frac{1}{2}\ln 2$, about an origin, defined at δ_C, by the discontinuous change from $T_V^{\mathrm{II}}=101$ K to $T_V^{\mathrm{I}}=108.4$ K. Hence, not only the intercept at the lowest observable first-order transition (i.e., 108.4 K), but the slope (i.e., $\frac{1}{2}\ln 2$) of the graph of $(K_1^{\mathrm{I}}-K_1^{\mathrm{II}})^{-1}$ vs T are fully determined. Unlike ΔK_1, the quantity $(K_1^{\mathrm{I}}-K_1^{\mathrm{II}})$ is obtained entirely from measured properties and requires no other reference. The quantitative agreement between the data and the topological constraint is evident in Fig. 6.

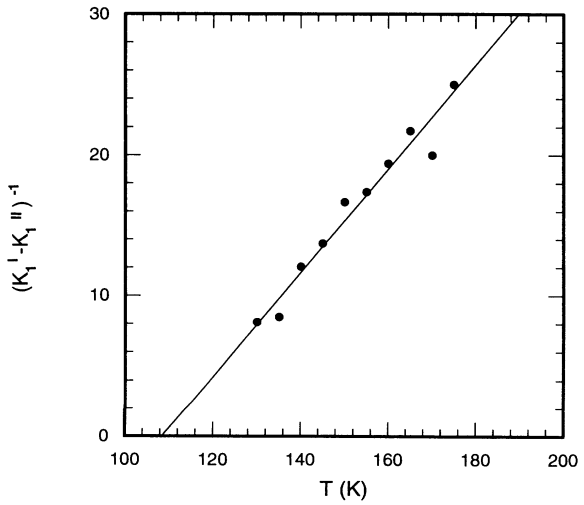

FIG. 6. Inverse of the difference of experimental K_1 values for $\delta=0.000$ and $\delta=0.006$ (circles) and predicted dependence with 108.4-K intercept and slope of $\frac{1}{2}\ln 2$ (solid line).

IV. CONCLUSIONS

The thermal dependence of the cubic magnetocrystalline anisotropic energy of magnetite crystals, with first-order ($\delta<\delta_C$) and second-order ($\delta>\delta_C$) Verwey transitions, reduces consistently with the topological constraints obtained from bifurcation analysis of a simple mean-field equation of state [cf. Eq. (5)]. The divergence of K_1^{I} from K_1^{II} below 250 K results from the splitting of excited electronic states with twice the degeneracy of the ground states in the first-order regime. It can be shown[21] that the observed characteristic temperatures of 81 K for the lowest T_V and 108 K, at the δ_C discontinuity between $T_V^{\mathrm{II}}=101$ K and $T_V^{\mathrm{I}}=108.4$ K, correspond to the Ising-model limits for the summation of pertinent exchange parameters over nearest neighbors in each regime.

A similar dependence, observed for the c_{44} elastic modulus,[15] is a necessary consequence of typicality, namely, of the universal character of the equation of state [Eq. (5)]. Empirical formulations of an order parameter may be obtained in terms of any equilibrium physical property. However, it is not the magnitude of the order parameter, but that of its first and higher derivatives with respect to the control variables which define criticality. The value of bifurcation analysis is that it provides an algorithm to identify the appropriate controls and map all empirical order parameters, in terms of unique essential variables, to the corresponding critical manifold.

Hence the reciprocal of the difference of c_{44}, measured for first- and second-order T_V samples, should vanish identically at 108 K with a slope of $\frac{1}{2}\ln 2$. The remarkable linearity of this type of graph (cf. Fig. 6) is noteworthy, because strong equivalence preserves the direction away from the nose of the cusp (i.e., the control coordinates for $\delta_C, l=t=0$), but not necessarily the curvature,[22] which depends on higher derivatives with respect to the control variables l and t.

It is inherent to the limitations of the mean-field approximation that its success in characterizing the Verwey-ordering contribution to free energy and, hence, to the thermal dependence of all equilibrium properties does not extend to the nature of the ordering mechanism. The most direct experimental evidence for this microscopic description is probably found in the diffuse scattering observed by electron[23] and neutron[24] diffraction between 200 K and T_V. Persuasively, the inverse of its intensity extrapolates to zero at ~ 108 K, although, in the absence of data for the second-order regime, the necessary reference to scale the ordinate of the graph is unavailable. The energy spectrum of this diffuse scattering has been interpreted[24] in terms of a pseudospin-phonon coupled system;[25] however, optical-phonon–magnon interactions in ferrimagnetic insulators yield similar expres-

sions for the differential scattering cross section[26] without further assumptions, if low-lying excited electronic states are admixed into the ground state by an oscillating crystal field.[27] The ensuing modulation of the exchange integral would then constitute the driving parameter for electronic ordering.

ACKNOWLEDGMENTS

The generous cooperation of Dr. Richard Harlow and Lou Lardear in providing access to the real-time Laue backreflection instrument at the Du Pont Experimental Station is gratefully acknowledged.

[1]In addition to subsequent citations in context, representative examples of early work include the following: H. J. Williams, R. M. Bozorth, and M. Goertz, Phys. Rev. **91**, 1107 (1953); C. H. Domenicali, *ibid.* **78**, 458 (1950); B. A. Calhoun, *ibid.* **94**, 1577 (1954); W. Palmer, *ibid.* **131**, 1057 (1963); Y. Syono, Jpn. J. Geophys. **14**, 73 (1965).

[2]E. J. Verwey and P. W. Haajman, Physica (Utrecht) **8**, 979 (1941).

[3]J. P. Shepherd, R. Aragón, J. W. Koenitzer, and J. M. Honig, Phys. Rev. B **32**, 1818 (1985).

[4]Z. Kakol, R. N. Pribble, and J. M. Honig, Solid State Commun. **69**, 793 (1989); Z. Kakol and J. M. Honig, Phys. Rev. B **40**, 9090 (1989).

[5]H. R. Harrison and R. Aragón, Mater. Res. Bull. **13**, 1097 (1978).

[6]R. Aragón, D. J. Buttrey, J. P. Shepherd, and J. M. Honig, Phys. Rev. B **31**, 430 (1985).

[7]Cf., for instance, F. Brailsford, *Physical Principes of Magnetism* (Van Nostrand, London, 1966), p. 121.

[8]Brailsford, Ref. 7, p. 133.

[9]For the numerical method, cf. W. H. Press, B. P. Flannery, S. A. Teukolsky, and W. T. Vettering, *Numerical Recipes* (Cambridge University Press, Cambridge, England, 1986), p. 515, implemented with S. Wolfram, *Mathematica,* 2nd ed. (Addison-Wesley, Reading, MA, 1991), p. 110.

[10]K. Abe, Y. Miyamoto, and S. Chikazumi, J. Phys. Soc. Jpn. **41**, 1894 (1976).

[11]The reasons for this discrepancy are unclear; however, subsequent experiments with the same instrumentation and samples comparable to those used in Ref. 4 agree within experimental error with those reported here; J. W. Koenitzer (private communication).

[12]Cf., for instance, L. R. Bickford, Phys. Rev. **78**, 449 (1950).

[13]J. C. Slonczewki, Phys. Rev. **110**, 1341 (1958).

[14]D. O. Smith, Phys. Rev. **102**, 959 (1956).

[15]S. Chikazumi, in *Magnetism and Magnetic Materials (Philadelphia, 1975),* Proceedings of the 21st Annual Conference on Magnetism and Magnetic Materials, edited by J. J. Becker, G. H. Lander, and J. J. Rhyne, AIP Conf. Proc. No. 29 (AIP, New York, 1976), p. 382.

[16]For the empirical use of the Curie-Weiss law, cf. E. V. Babkin, N. A. Drokin, K. P. Koval', and V. G. Pyn'ko, Fiz. Tverd. Tela (Leningrad) **26**, 1493 (1984) [Sov. Phys. Solid State **26**, 905 (1984)]; for the generalized behavior of the order parameter around the critical point, cf. T. Poston and I. Stewart, *Catastrophe Theory and its Applications* (Pitman, London, 1978), p. 331.

[17]R. Aragón and J. M. Honig, Phys. Rev. B **37**, 209 (1988).

[18]S. Strässler and C. Kittel, Phys. Rev. **139**, A758 (1965).

[19]Cf. Ref. 17 for proof of Eq. (6) from bifurcation theory and the values of g_1/g_0.

[20]The only condition is that diffeomorphic invariance be preserved; cf. Poston and Stewart, Ref. 16, p. 339.

[21]The relation between transition temperatures and exchange interactions is addressed in R. Aragón, preceding paper, Phys. Rev. B **46**, 5328 (1992).

[22]Cf. Poston and Stewart, Ref. 16, p. 338.

[23]K. Chiba, K. Suzuki, and S. Chikazumi, J. Phys. Soc. Jpn. **39**, 839 (1975).

[24]S. M. Shapiro, M. Izumi, and G. Shirane, Phys. Rev. B **14**, 200 (1976).

[25]Y. Yamada, H. Takatera, and D. L. Huber, J. Phys. Soc. Jpn. **36**, 641 (1974); K. N. Pak and W. Kinase, *ibid.* **38**, 1 (1975).

[26]A. W. Joshi and K. P. Sinha, Proc. Phys. Soc. London **91**, 97 (1967).

[27]For a review, cf., for instance, K. P. Sinha and N. Kumar, *Interactions in Magnetically Ordered Solids* (Oxford University Press, New York, 1980), p. 101.